

First principles study of Tritium-doped Lithium-Lead liquid alloy: structure and diffusion

JOËL MARTÍN DALMAS
Universidad de Valladolid

L.E. GONZÁLEZ AND D. J. GONZÁLEZ

September 24, 2020

Abstract

In this article, we will discuss the behaviour of the atoms that constitute the blanket part of TOKAMAK fusion reactors breeder, through of Ab initio molecular dynamics simulations. One of the proposed materials to constitute this blanket is the eutectic LiPb liquid alloy. In our simulations, we considered a system formed by Lithium and Lead and we have also included Tritium atoms to perform a more accurate modelling. Representing the system by four different thermodynamic conditions, varying the amount of Tritium dissolved and the density (or pressure) we were able to compare and carry out a wide study about the properties of the system. In the first place, we studied the statical magnitudes of the three-component liquid. We were able to appreciate the formation of Tritium molecules, so it was necessary to change the analysis of our system to that of a four-component liquid (Li, Pb T atoms and T₂ molecules). We considered the atomic organization of the system by studying the way that the different components are distributed around each type of atom/molecule. After that, we also worked on the dynamical magnitudes, obtaining the diffusion coefficient of the different atoms and also their vibrational frequencies. In the particular case of the T atoms, we could verify that the vibration frequency of the T₂ molecule provides an appreciable signal to the spectrum, and how their interaction with Li atoms modifies these frequencies.

En este artículo se van a emplear simulaciones Ab initio de dinámica molecular para estudiar el comportamiento de los átomos que constituyen la parte del "blanket" en los reactores de fusión tipo TOKAMAK, que cumple la función de "breeder". Puesto que uno de los principales materiales propuestos para constituir el blanket se trata de la aleación líquida de LiPb en su punto eutéctico, en nuestra simulación se ha considerado un conjunto de átomos formado por litio, plomo y también tritio, para de esta manera conseguir un modelado más preciso. Variando las propiedades termodinámicas de presión y número de tritios en el sistema, se ha conseguido realizar un amplio estudio de las propiedades del sistema a través de cuatro simulaciones con diferentes condiciones. En primer lugar se estudiaron las propiedades estáticas del sistema, a través de las cuales se dedujo que en el interior de la simulación se formaban moléculas de tritio. Este descubrimiento hizo necesario cambiar la organización de la simulación y pasó a tratarse como un sistema de cuatro componentes (Li, Pb, átomos de T y moléculas de T₂). Estudiando como se distribuían las diferentes componentes unas con otras mediante funciones de densidad radial pudimos estudiar la organización estructural del sistema. Una vez hecho esto, pasamos a analizar las variables dinámicas de las simulaciones, obteniendo los valores de los diferentes coeficientes de difusión y de las frecuencias de vibración de los átomos. En el caso particular de los átomos de tritio, se pudo observar cómo en el espectro de las frecuencias de vibración aparece modificado por la aparición de un leve pico de frecuencias de vibración moleculares.

I. INTRODUCTION

The energy production in Fusion Power Plants (FPP) is based on a simple reaction: $D + T \rightarrow He + n$. This reaction occurs inside the reactor plasma and requires Deuterium and Tritium to produce Helium, one neutron and 14.1 MeV, which are mostly taken as neutronic kinetic energy. The Tritium used as fuel does not exist naturally in a sufficient amount, but fortunately it can be produced artificially (that is, through breeding) inside the FPP. This Tritium breeding is one of the functions of the Blanket part of the reactor [1]. The most useful breeding reaction is obtained by neutron collision with the lithium nucleus ($Li^6 + n \rightarrow T + He$).

For this reason, the use of Lithium or some compounds that contain it is mandatory in the Blanket of the FPP [2].

There are several features in liquid metals that make them attractive candidates for fusion applications. Mainly, we have to consider their potential to work at low pressure, which is a safety advantage. Also, the liquids are immune to radiation damage and thanks to the blanket, for being a liquid, the Tritium can be circulated, so there is a bigger flexibility for Tritium removal [3]. Pure liquid Li, however, shows several shortcomings for its direct use, the most serious one being its high reactivity, in particular with water.

Note however that pure liquid Li is nevertheless still considered as a candidate for breeding material. Li compounds are more promising as breeders, either in solid ceramic form or as liquid metals. The presence of atoms other than Li, hinder the chances of neutrons being absorbed by the Li atoms; consequently neutron multipliers, which absorb one neutron and emit two of them, are required for proper operation. The most adequate neutron multipliers are Be and Pb, through the (endothermic) reactions $\text{Be}^9 + n \rightarrow 2 \text{He}^4 + 2 n$, and $\text{Pb}^{208} + n \rightarrow \text{Pb}^{207} + 2 n$.

There are, therefore, mainly two different types of materials proposed to fulfill the blanket function: the one is based in the use of beryllium, typically Li_4SiO_4 or $\text{LiTiO}_3 + \text{Be}$ or Be_{12}Ti in the form of pebble beds, and the second one which is a type of blanket material based on liquid LiPb alloys [4]. In particular, the eutectic composition $\text{Li}_{17}\text{Pb}_{83}$ is favoured, being the one with the lowest melting point. In principle, being a liquid with high thermal conductivity makes it also possible to use it as coolant (which is other of the functions of the blanket). There are, however, some inconveniences for this use: one of them is the magnetohydrodynamic effects due to the large magnetic fields that are present in the reactor, which hinder an efficient flow of the liquid metal, and the second one is the high flow velocity needed for an efficient heat extraction. For this reason, an additional component is being considered as coolant, which is easier to manage, the two candidates being He and water.

At present, therefore, there are four different types of test blanket modules whose capabilities will be studied at ITER, with the aim of selecting the best candidate for its use in DEMO [5]. These are the He cooled pebble bed (HCPB) one, the water-cooled LiPb (WCLL) [6], design, the He cooled LiPb (HCLL) module [7] and the dual cooled LiPb (DCLL) one [8], where He is used to cool the whole system but the liquid LiPb allow helps in its self-cooling.

In this work, we will focus our attention on the eutectic LiPb liquid alloy, as it fulfils correctly the three requisits that the material has to accomplish [9]. It acts as a breeder, as a neutron multiplier and it also acts as a good self-cooling system. Besides that, another additional benefit that this alloy has is the lowest melting temperature at the eutectic composition [10]. Finally, we mention another advantage of the eutectic alloy, namely, its lower tritium solubility as compared with pure Li [11], which makes easier the tritium extraction for further injection in the plasma. That is why this material stands among the most promising candidates [10].

The material of study of the present research is a mixture between the atoms that compose the alloy (Li and Pb in the proportion of the eutectic alloy) that constitutes the blanket and the tritium that has to appear due to the breeding reactions. With

this composition, the description of the simulation is expected to be closer to the real behaviour. Of course, a He atom also appears at every breeding reaction and an even more representative situation would require to include it (in the same amount as Tritium) in the study. This is left for future research, but we must note that the expected effects of the dissolved He in the liquid LiPb eutectic is the possible formation of He bubbles (depending on the pressure conditions of operation) which should be extracted for proper operation [12].

The properties of liquid Li-Pb alloys at several compositions have been studied through a few experimental researches [13] [14]. In fact this system is also interesting from a scientific (not only technological) point of view, since the type of interaction between Li, Pb and electrons, shows important variations as a function of composition [15]. For example, pure Li and pure Pb are metals, but Li_4Pb is a quasi-ionic liquid compound due to charge transfer between Li and Pb. Some properties, like the volume per atom deviates strongly from the ideal behaviour [13], but at the same time, other important relations, like the Sievert's law are well fulfilled ([11] [16]). Also, the liquid structure has been measured through neutron diffraction for several compositions [17]. Despite the lack of additional technological applications other than nuclear fusion technology, recent efforts are focused on the creation of an extended database of materials properties for the eutectic alloy [18]. The solubility of hydrogen and its extrapolation to tritium is a key factor in the blanket's design and development. Sievert's law states that the atomic solubility (maximum atomic concentration dissolved in the liquid) of a diatomic gas is proportional to the square root of the vapor pressure of the gas above the liquid's surface, $c = K_s P^{1/2}$. The Sievert's constant, K_s , has been reported by several authors as a function of temperature. The results obtained for this magnitude showed a lower tendency to absorb the hydrogen atoms in $\text{Li}_{17}\text{Pb}_{83}$ than in pure lithium [11]. This is a favourable factor for the alloy, because a lower absorption of tritium makes easier its extraction. However, there is a huge variability between different experiments (by orders of magnitude) most probably due to the inherent difficulty in this type of measurements prone to many parasitic effects [19].

Another critical factor is the diffusion constant of tritium in the alloy. This has been compared through various experiments ([20], [21], [22]) with the value of pure liquid lithium ([23], [24]). The results revealed a higher value of the diffusion constant in the first case, indicating a bigger mobility of the hydrogen isotopes in the eutectic alloy. In any case, the measurements are rather indirect (mainly from hydrogen release out of a liquid sample contained in a tube), and the value of the diffusion coefficient is obtained by following different models of hydrogen transport through the liquid metal, through the material of the containing tube, recombination at the outer surface and so on. Consequently,

there is some degree of uncertainty in the measurement [25], and different authors produce different correlation formulas for the diffusivity in term of temperature and activation energies.

Moreover, there is no experimental information about the diffusivity of the lead and lithium atoms. In this work, we have considered this question, and we have made a study concerning the compared mobility of the three different types of atoms.

The difficulty in the experiments that we have briefly discussed before showcases the convenience of other research methods where the system to study is fully under the researcher's control. At this point is where atomistic simulations play an important role. In a simulation, no unwanted impurities are present, the thermodynamic state is precisely defined, the structure can be easily obtained and the motion of the different atomic components can be specifically followed, providing very detailed information that in many cases is out of reach for experiments. The "only" requirement for this method is an adequate description of the interactions among the atoms composing the system. The adequacy of the interactions can only be judged based on a comparison between simulation results and experimental measurements, whenever these are available.

The requirement of good atomic forces is not trivial, and remarkable efforts are required to develop interatomic potentials that describe these interactions realistically. For the particular case of the LiPb eutectic, we mention some recent work by Alberto Fraile [12] built upon previous development of a semiempirical potential by David Belashchenko ([26] and [27]) and Wu [28]. Besides, very recently a study has been published including also He atoms in the liquid eutectic alloy, by modelling their interaction with other He atoms, with Li atoms and with Pb atoms through simple Lennard-Jones pair potentials [29].

Another type of computational approximation to achieve a correct description of the interactions is the use of first-principles molecular dynamics, where the forces are obtained from explicit electronic structure calculations. This is much more precise than semiempirical models, but it is computationally much more demanding. As a consequence, the number of atoms that can be included in the simulations is much smaller. Investigations of the pure eutectic LiPb alloy using this kind of simulations are not published yet. But curiously, using this method, Daisuke Masuyama et al [30] simulated an eutectic alloy of LiPb composed of 36 atoms and one additional single hydrogen atom. This way, they could study the H atom movement through the liquid to elucidate the chemical state of the hydrogen and the mechanism of hydrogen diffusion. The calculation showed a tendency of the hydrogen to bind with lithium atoms; this means that the diffusion of the hydrogen is produced by jumping from one lithium to another.

In our study, we have increased substantially the number of atoms included explicitly in the simulation, using 256 atoms corresponding to the lithium-lead alloy, and a variable number of tritium atoms inside the sample, and performed first-principle molecular dynamics. By studying the system at an atomic level, we have been able to perform a precise analysis of some of its physical properties. Having a larger sample and multiple tritium atoms allows us to perform a bigger and more precise analysis than the one done by Masuyama group [30]. This allows us to observe the interactions between tritiums and their direct consequences in the other atoms and the whole modelled system. This work is, in fact, a continuation of a previous research where we included 256 atoms of the alloy plus 64 tritium atoms [31]. That study, however, was performed by using a density that turned out to correspond to a large pressure. In this study, we have varied the densities for all of the studied compositions, so that the resulting pressure is reduced to a few kbars. Moreover, we will also report here on yet unpublished results, previously obtained by Luis E. Gonzalez and David J. Gonzalez in collaboration with other researchers, on first principles simulations of the pure eutectic liquid alloy, i.e. with no tritium at all, which is part of a more comprehensive study of Li-Pb liquid alloys at several atomic compositions [32]. By comparing several cases with different physical conditions, it is possible to extract information about how these conditions influence our system.

In this work, we have analysed both static and dynamical magnitudes of the atoms. These magnitudes are the radial density functions, being $g(r)$ the pair correlation function and the $G(r)$ the radial distribution function, we also studied the vibrational frequencies, f , the mean squared displacements (MSD), $\delta r^2(t)$, the velocity autocorrelation function (VAF), $Z(t)$, and the diffusion coefficient, D , which can be obtained from either of the two previous magnitudes.

II. TECHNICAL DETAILS

We have performed first principle molecular dynamics simulations (FPMD) for a ternary system composed of lithium, lead and tritium atoms. The simulation parameters of the different studied cases are shown table 1. As it can be seen in the table, the temperature selected for all the cases was 775 K, which was motivated by the possibility to compare the structural results obtained for the pure eutectic alloy with the experimental ones of Ruppertsberg and Egger [17], so as to check the correct description of the interatomic interactions. This temperature is also interesting to our simulations cause it is not too far from the melting point of the alloy but not too close to it either (which could lead to spurious solidification in some cases). The eutectic melting point, 508 K is one of the few parameters of the PbLi alloy where there is a general agreement between the different works [11, 33, 34, 35, 36].

System 1 corresponds to our earlier study with 64 T

atoms [31], that led to high values of the pressure. For system 2 the volume of the simulation box has been increased in sufficient amount so as to obtain a small positive pressure. In the case of system 3 the amount of T has been reduced by a factor of 2, while the volume of the simulation box has been readapted to provide an acceptable value of the pressure. Finally, system 4 corresponds to the pure eutectic alloy with no tritium atoms [32].

To achieve the equilibrium state of the simulations, we had to perform a previous thermalization process in which the energy of the system was let free to evolve, while the atomic velocities were rescaled so as to obtain the desired temperature, until a stable state is achieved. We judge the stabilization by the lack of drift in the energy (and pressure) of the system. When such regime is obtained the energy will fluctuate around an average value.

It is interesting to note here that multicomponent systems, especially when they include components with very different masses, can take quite long to reach equilibrium, depending on the starting configuration. We have explicitly checked that the configurations used for the calculation of properties correspond to the equilibrium state, and discarded the (large number of) timesteps during which the equilibration phase took place.

The FPMD simulations were performed using the VASP [37] code. This is a density-functional-theory (DFT) based program. For the exchange-correlation energy we used the PBE generalized gradient functional [38] and for the electron-ion-core interaction, we used the projector augmented wave (PAW) potentials [39] provided by the VASP developers in the distribution of the program. The orbital configuration taken for the different atoms is the one from the neutral atoms. The plane-wave cutoff energy was set to 29.4 Ryd, which is the largest one recommended by the developers of the PAW potentials for the three elements. We used cubic supercells with a variable number of atoms that goes from 256 to 320 with periodic boundary conditions, including 43 atoms of lithium, 213 atoms of lead and a variable number of tritium atoms. For the computation of energies and forces, we used Brillouin-zone integrations by taking only the Γ point, which is justified by the relatively large size of the simulated system. After the equilibration process, we performed a number of equilibrium configurations N_c as given in table 1, with a time step of 1 fs, so our simulation time varies between 22.585ps and 38.787ps.

Note that a small timestep is required because of the small value of the atomic mass of T. On the other hand this means that Pb atoms (70 times heavier) will need many timesteps to move appreciably.

The simulations of the pure eutectic alloy were performed using the PARSEC code, a real space implementation of DFT, with norm-conserving pseudopotentials optimized for the two atomic species. The total number of particles was slightly smaller in this

study, amounting to 42 Li atoms and 205 Pb atoms [32].

As it has already been told in the introduction, there are only four simulation studies concerning the blanket material at the eutectic point, and only one of them uses a first principle method, like ours. This FPMD study [30] considered a composition of 6 Li atoms, 30 Pb atoms and 1 H atom, instead of tritium, as it has a greater mobility so that they could analyze the diffusion in a faster way. The physical conditions in this case were a temperature of 900 K and a 10.5 Å size for the cubic simulation cell. They used the CASTEP code [40] in the MD simulations (also based on DFT) with GGA-PBE functionals and ultrasoft pseudopotentials. The time step was set to 1 fs and they achieved 1000 configurations, so the total time was 1 ps.

Thus it is clear that our calculations will provide a lower statistical error, because the simulations were done with a larger amount of atoms and during a longer total simulation time. We also calculated other parameters not available in the previous literature. Particularly, this is the first research concerning the PbLiT alloy that studies the variation in structural and dynamical properties of the Li and Pb atoms, under the influence of the amount of tritium present. Additionally, comparing the results of systems 1 and 2, the influence of pressure on the properties can also be analyzed.

The use of multiple tritium atoms is also an important point for an additional reason. In principle it is expected that T will appear in atomic form, mostly bound to Li atoms (as observed by Masuyama and coworkers). However, when more than one tritium atom is present in the system, one should not preclude the possibility of formation of T_2 molecules (i.e. T-T bonds may compete with T-Li bonds) and, as we will see later, this is an important phenomenon that indeed occurs during the simulation. Such molecules live transiently, so that they form and break after some time. But nevertheless we have found that a finite non-zero number of molecules are present in the system at every timestep, and consequently we have analyzed also their atomic distribution and some of their dynamic properties, in particular their vibration frequency, and how this is affected by the amount of T present and by the pressure. Note that this implies that our system can be considered as containing in fact four components rather than three, namely, Li atoms, Pb atoms, T in atomic form and T_2 molecules. This has of course a direct impact in the equilibration time, but also means that the structure must be analyzed with more detail leading to an increased number of pair distribution functions, changing from 9 types of pairs (or six if we used the symmetric form) to 16 types (ten in the symmetric form).

Table 1: Physical properties of the four different studied systems.

System	$L(\text{\AA})$	$\rho(\text{\AA}^3)$	$P(\text{Kbar})$	N_c
1- 64 H	18.5212	0.05037	150	29600
2- 64 H	20.2069	0.03878	18	22585
3- 32 H	20.1069	0.03543	13	38787
4- 0 H	19.6569	0.03252	≈ 0	28200

III. RESULTS

Our study is focused on several static and dynamic magnitudes. Two of them are structural properties, $g_{ij}(r)$ and $G_{ij}(r)$, and they are both two types of radial density functions. The (partial) pair correlation function, $g_{ij}(r)$ represents the probability density of finding a neighbour of type j at a (radial) distance r of an atom of type i . For homogeneous liquids, it is symmetric under the interchange of labels, so $g_{ji}(r) = g_{ij}(r)$. The (partial) radial distribution functions, $G_{ij}(r)$ take into account additionally the volume of the spherical shell of radius r and the number of atoms of type j that would be contained in such a volume if they would be uniformly distributed. We can write, then, that $G_{ij}(r) = 4\pi r^2 \rho x_j g_{ij}(r)$, where x_j is the atomic fraction of component j , and ρ is the number density. Therefore a simple integration of $G_{ij}(r)$ between $r = 0$ and $r = R$ allows us to quantify the number of neighbours of type j around an atom of type i within a distance R . Note, however, that the presence of the atomic concentration of component j in the definition rules out the symmetry (unless all atomic fractions would be equal). Finally, we also mention the total radial distribution function of atoms around an atom of type i , $G_i(r)$, which is given by the sum of all the partial $G_{ij}(r)$ for all possible values of j . That is, it describes how atoms, irrespective of its type, are distributed around an atom of type i , and its integral from $r = 0$ to $r = R$ is the total number of neighbours within a distance R around an atom of type i .

Regarding dynamic properties, we have calculated the MSD and the VAF. The MSD measures the average (squared) displacement of an atom as a function of time, and the VAF represents the average projection of the velocity of an atom over its initial velocity as a function of time. In both cases, the averages are taken with respect to particles of the same type and over time origins. Both of these functions are useful to obtain the diffusion coefficient, D (for each type of component), which is one of the paramount dynamical magnitudes, as it measures the mobility of an atom. The last studied magnitudes are the vibrational frequencies of the atoms, f , which are obtained from the Fourier Transform of the VAF.

In the following, to illustrate the type of results obtained, we will show the data corresponding to system 3, i.e. to that with 32 tritium atoms. Then we will discuss the variation with pressure and tritium content globally.

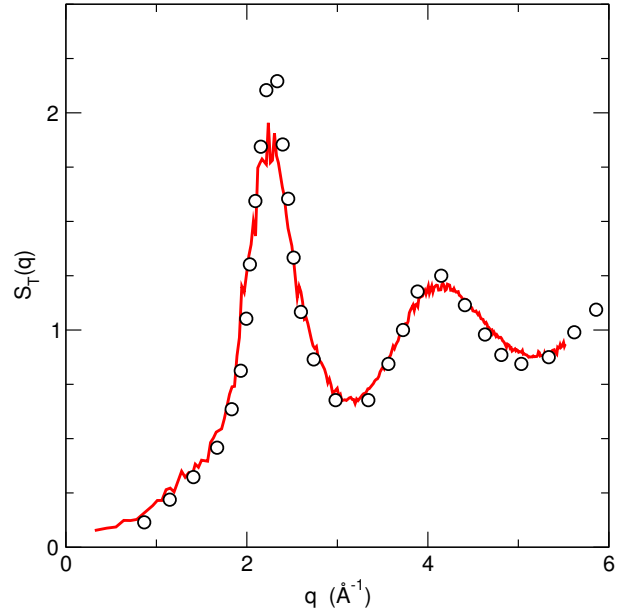


Figure 1: Neutron weighted total structure factor, $S_T(q)$, of liquid $\text{Li}_{0.17}\text{Pb}_{0.83}$ at 775 K. Symbols: experimental data. Line: simulation results.

i. Are the interactions described correctly?

As mentioned above, it is vital to describe correctly the interatomic interactions if we want to have confidence in the results obtained from simulations. The accuracy of first-principles calculations is intrinsically very high. Nevertheless some approximations are always introduced in the process, and therefore a comparison between simulation results and experimental measurements for some magnitudes (if successful) reassures that the predicted results, for which no experimental data exist, are really meaningful.

In the case of the LiPb eutectic alloy, the structure has been measured by neutron diffraction [17]. Neutrons sent towards the liquid sample interact with the atomic nuclei, and the coherent scattered radiation for a given angle is proportional to the so-called neutron weighted total structure factor, $S_T(q)$. This function is a linear combination of the partial structure factors, $S_{ij}(q)$, which are related to the Fourier Transforms of the partial pair correlation functions [41]. The coefficients of the linear combination include the atomic fractions and the neutron scattering length of each type of nucleus in the alloy.

In figure 1 we show the results obtained for the pure eutectic alloy (with no tritium) from the simulation study and the measured data. There is an excellent agreement between them, and consequently the rest of magnitudes reported here are expected to be a good representation of those of the real liquid.

ii. Structural properties

The pair correlation functions $g_{ij}(r)$, of the different atoms, obtained for the 32 H case are depicted in the

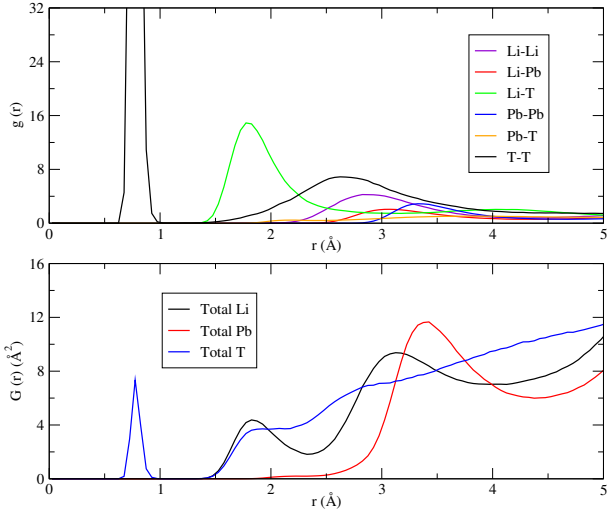


Figure 2: Radial density functions of the three-component system of the third simulation state (3-32H) at 775 K. The first graph corresponds to the partial correlation functions $g_{i,j}(r)$ of all the possible pairs. The lower graph corresponds to the total distribution functions $G_i(r)$ of the three types of atoms.

upper part of figure 2. This image plots the multiple correlation functions between the three types of atoms in the simulation. The shape of these functions is quite typical of liquid systems, halfway from perfect solids (regular delta functions ad infinitum) and gaseous systems (no oscillations). This shows a disordered state at long-range, but with enough short-range order to talk about first coordination shells and first neighbours, which are not at fixed distance, but instead distributed with a probability density. The second, third, and the consecutive coordination shells, continue towards a larger r , but are less and less defined (their distribution is wider and wider) as the distance increases. The maxima of the $g_{ij}(r)$ signal then the most probable distances where the neighbours would be found, and the minima can be taken as the (fuzzy) frontiers between coordination shells. In fact, it is usual to consider the maxima of $g_{ij}(r)$ to talk about most probable distances, but the minima of the partial $G_{ij}(r)$, or total $G_i(r)$ to talk about the frontiers of the coordination shells, and we will follow this criterion throughout.

The total pair distribution functions around the three types of atoms, $G_i(r)$, are shown in the bottom part of figure 2. The three cases show a clear first peak which corresponds to the first neighbours, but the tritium one is located at a very short distance and is quite sharp as compared to the other atoms. On the contrary, the second coordination shell of T atoms looks similar to the first coordination shell of Li and Pb atoms.

This particular first peak of $g_{T,T}(r)$ stands out of the other results, and its location at a distance lower than 1 Å made us suspect about the formation of tritium molecules T_2 inside the blanket since this is comparable

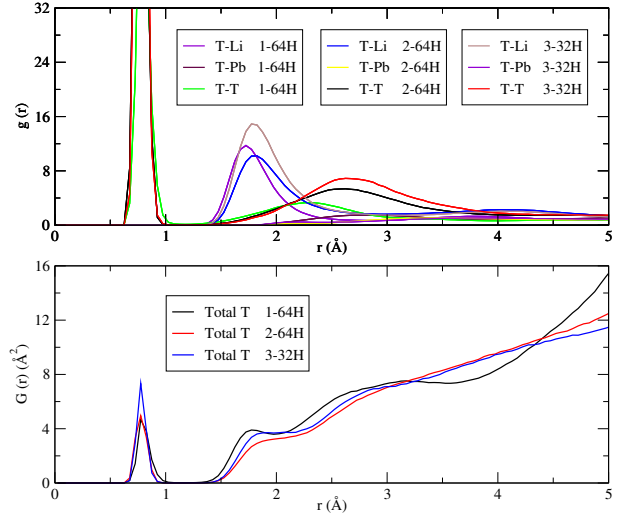


Figure 3: Comparison between the radial density functions of the three-component system at 775 K of first three different simulational cases. The first graph corresponds to the partial correlation functions $g_{i,j}(r)$ of all tritium relations. The lower graph corresponds to the total distribution functions $G_i(r)$ of the tritium atom in the three cases.

with the equilibrium distance of the hydrogen molecule. The situation is similar for the other systems that contain tritium (systems 1 and 3). There are differences in other properties, but the first peak of $g_{T,T}(r)$ at less than 1 Å is present in all the cases, as it is shown in figure 3.

Looking at the decomposition of tritium’s total correlation function, into its different parts, $g_{T,T}(r)$, $g_{T,Li}(r)$ and $g_{T,Pb}(r)$ (figure 4), it is easy to see that, indeed tritium is the only atom that contributes to the first peak, whereas all different components contribute to the later shells.

A visual inspection of the evolution of the atomic configurations confirmed the existence of pairs of tritium atoms close together rotating and vibrating (and translating, of course). Consequently, we proceeded to modify the programs to study a four-component system, made up of Li atoms, Pb atoms, T atoms and T_2 molecules.

We considered a pair of atoms to be “bonded” in a T_2 molecule when their distance is lower than 1.26 Å, which is the location of the first minimum of $G_{T,T}(r)$. This is certainly not a good definition for a chemically bonded molecule and indeed, we have found cases of tritium atoms not bonded in a molecule that collide with each other and then depart from one another, and during a short amount of time are within the chosen distance to define them as “a molecule”. These cases are, however, not frequent; and the only effect they will have is the introduction of some additional noise in the statistical description of properties related to T_2 molecules.

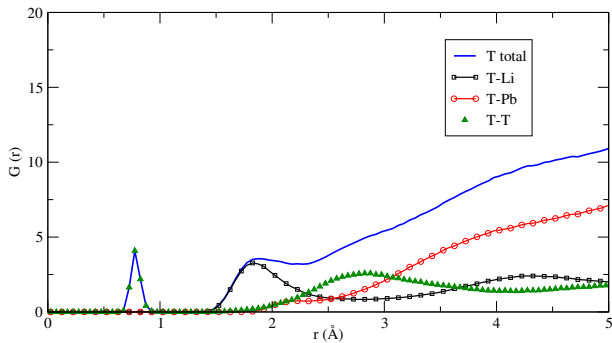


Figure 4: Relations between lithium and all the atoms of the three-component system of the third simulational case (3-32H) at 775 K.

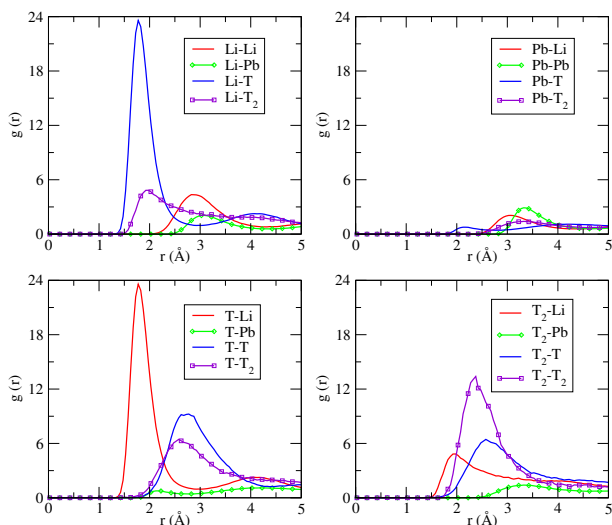


Figure 5: Pair correlation functions $g_{i,j}(r)$, of the tetra-component system of the third studied case (3-32H) at 775 K.

In order to describe the distribution of T_2 molecules in the system, we used their centres of mass as their characteristic location, so when we later talk about $g_{Li,T_2}(r)$ (for example) it must be understood that we are talking about the partial pair correlation function between Li atoms and the centers of mass of T_2 molecules.

Analysis in terms of four components

Figure 5 displays all the pair correlation functions of the new tetra-component system for the case of 32 H. We can observe in the figure a typical pair distribution function behaviour in all the components, including the T_2 molecule. The result of the transformation is similar in the other simulation cases that involve tritium.

Table 2 compares the most probable distance from an atom to its first neighbours and the height of the corresponding pair correlation function between the three-component and the four-component system in the 32H simulations. The main differences can be

Table 2: Characteristic parameters of the first peak of the $g(r)$ functions for every pair of atoms of the three and four component systems.

First neighbours				
Relation	3 Components		4 Components	
	Distance	Heigh	Distance	Heigh
LiLi	2.85	4.30	2.85	4.30
LiPb	3.075	2.06	3.075	2.06
LiT	1.775	14.76	1.775	23.57
Li T_2	-	-	1.95	4.83
PbPb	3.325	2.89	3.325	2.90
PbT	3.80	1.04	2.15	0.76
Pb T_2	-	-	3.325	1.40
TT	0.775	137.32	2.75	9.18
TT $_2$	-	-	2.575	6.44
T $_2$ T $_2$	-	-	2.375	13.39

observed in the relations where tritium is involved. The fact that some tritium atoms become molecules implies a major change in all of its pair correlation functions and the most clearest one occurs in the T-T partial. The first sharp peak disappears and the second peak of the 3-component system evolves to constitute the first peak of the four-component liquid.

Figure 6 shows the pair distribution functions, $G_{ij}(r)$ of all the different pairs of components for the system with 32 H. Also shown are the total pair distribution functions, $G_{Li}(r)$, $G_{Pb}(r)$, $G_T(r)$ and $G_{T_2}(r)$. The first minimum of these 4 functions denotes the extent of the first coordination shell for each component. Integrating these functions from the origin to the distance of the first minimum, we obtain the total number of neighbours in the first shell of the atom. Integrating in the same range the partial $G_{ij}(r)$ gives the decomposition of this total number of neighbours into those that correspond to each species. This information has great importance to understand the internal structure of the blanket. Furthermore, this is crucial to understand how do the atoms organize themselves and what are their first neighbours preference, which is also important to understand the chemical behaviour of the atoms.

In table 3, we show the integration ranges that enable us to compute the number of first neighbours of any atom, as reported in the table. Note that all the simulation cases are displayed to compare the different behaviour of the atoms when the thermodynamic parameters (number of tritiums and pressure) change.

Table 3 exhibits the general short-range distribution of the atoms at a structural level, from which we can extract some interesting information concerning the first neighbours. In all the cases that contain tritium

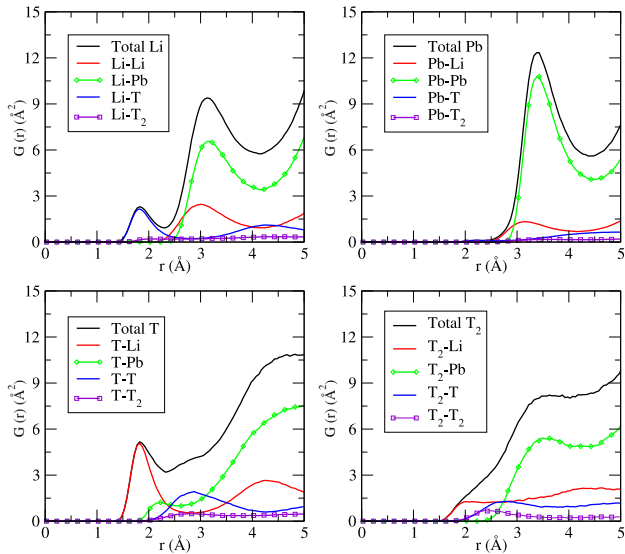


Figure 6: Radial distribution functions $G_{i,j}(r)$, of all the possible pairs of the tetra-component system of the third simulation case (3-32H) at 775 K.

Table 3: Number of neighbours for every pair of atoms within a distance given by the first minimum of the total distribution function $G_i(r)$ of a given type of atom.

1 - 64H						
Distance	Atom	Total	Li	Pb	T	T ₂
2.18	Li	1.71	0.03	0.00	1.31	0.38
4.13	Pb	14.21	1.74	10.68	0.90	0.92
1.98	T	2.23	2.06	0.07	0.05	0.06
2.17	T ₂	1.26	0.79	0.00	0.16	0.30

2 - 64H						
Distance	Atom	Total	Li	Pb	T	T ₂
2.28	Li	1.59	0.03	0.00	1.34	0.23
4.43	Pb	11.68	1.47	9.99	0.62	0.76
2.28	T	3.12	2.62	0.31	0.09	0.10
-	T ₂	-	-	-	-	-

3 - 32H						
Distance	Atom	Total	Li	Pb	T	T ₂
2.33	Li	1.21	0.02	0.00	1.07	0.11
4.48	Pb	12.82	1.69	10.22	0.66	0.26
2.38	T	3.25	2.57	0.47	0.14	0.07
-	T ₂	-	-	-	-	-

4 - 0H				
Distance	Atom	Total	Li	Pb
4.22	Li	10.32	1.13	9.20
4.23	Pb	10.84	1.92	8.91

Table 4: Distance to first peak and number of first Li neighbours for tritium molecules in systems 1, 2 and 3.

Relations between T ₂ and Li		
Simulation	d (Å)	$n_{T_2, Li}$
1- 64H	1.78	1.10
2- 64H	2.15	0.62
3- 32H	2.08	0.81

atoms (systems 1, 2 and 3) the first neighbours' shells of the different components have the same qualitative properties. Li atoms are surrounded in their first shell mainly by atomic tritium, and to a smaller extent by molecular tritium. The significant first neighbours for lead are other lead atoms, followed by a much smaller amount of Li atoms. In the case of atomic tritium, the main components of the first coordination shell are lithium atoms. However, in the two cases with lower pressure, the total pair distribution function, $G_{T_2}(r)$, of molecular tritium has not well-defined shells, as there are no minimums in the function. This is depicted in figure 7, where we also observe that for higher pressure (system 1) the minimum is clearly present at an approximate distance of 2.17 Å. Comparing the situation at low and high pressures, it seems that the second coordination shell overlaps strongly with the first one, which is indicating a higher degree of disorder. Nevertheless, we can extract some information about the local environment around tritium molecules by looking at the correlations between T₂ and Li, which are the ones that show features at shorter distances from the tritium molecules, as observed in figures 5 and 6. The $G_{T_2, Li}(r)$ functions show a maximum followed by a very weak minimum, so we can define several first Li neighbours, although with a high degree of uncertainty. The first peak is also quite weak, but in any case it is possible to track its position when the thermodynamic parameters change. The corresponding values are shown in table 4. We observe a small variation of the number of Li neighbours as a function of tritium content or pressure, but a significant change in the position of the peak. When pressure increases, the first Li neighbours of T₂ molecules are located closer to them. This data will be useful later when we study the vibrational frequencies of tritium molecules.

In fact, this same tendency is observed for all types of pairs. In table 3, we can observe that the extents of the first coordination shells of all the atoms decrease from system 2 to system 1, i.e., under the application of pressure. It is also interesting to note that pressure makes the system more structured, which higher and narrower peaks if the distribution functions. This was evident in figure 7 for $G_{T_2}(r)$, but it is a general feature for all the different pairs.

On the other hand, the variation with tritium content looks less marked (once tritium atoms are present) as follows from the comparison between system 2 and

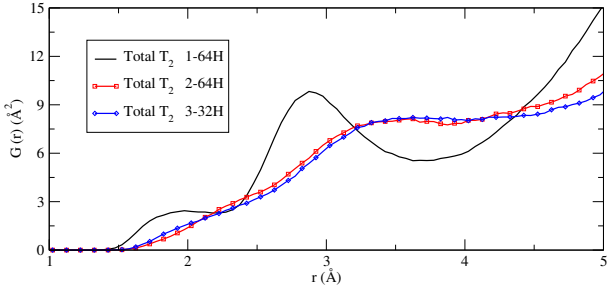


Figure 7: Total correlation functions $G_{T_2}(r)$, of the tritium molecules corresponding to the first three simulation states.

system 3, where we observe a small expansion of the first coordination shells when decreasing the number of tritium atoms present.

A final point to consider, concerning structural properties, is the change brought about by the presence of tritium in the structure of the underlying alloy, the LiPb eutectic. In figure 8 we plot the three pair correlation functions $g_{Li,Li}(r)$, $g_{Li,Pb}(r)$ and $g_{Pb,Pb}(r)$ as a function of T content. The latter function is almost unchanged, while the previous one changes drastically with an enormous increase in its height for the systems containing tritium. In order to understand this behaviour, we turn back to figure 5. There we observe that the Li-H partial pair correlation functions stand up because of its height. This indicates a strong interaction between Li and T atoms. As we mentioned in the introduction, this is in line with the first-principles study of Masuyama and collaborators, who moreover studied the charge that could be associated with the only H atom considered and interpreted it in terms of a strong ionic-like bond between Li and H. We have not analyzed the question of the charges (so to say, the chemical state) of the different atoms, but as we said we consider the Li-H interaction as being quite strong due to the characteristics of the corresponding distribution function. This strong interaction between Li and T somehow drives an increased Li-Li interaction mediated by the T atoms. This way the Li-Li interactions are enhanced and the distribution function increases accordingly.

We finish this section by considering the amount of molecular tritium observed in our simulations. It is important to realize that the configurations used for the analysis of the properties are by no means all of the configurations generated during the MD runs. Many other configurations were generated previously for equilibration before we reached an equilibrium state. MD simulations start from an initial atomic configuration, with appropriate velocities, and then the system evolves under the action of the atomic forces.

For the initial configuration, we took a crystalline structure composed of Li and H with 256 Li atoms and 64 H atoms. In this structure, no molecules existed and

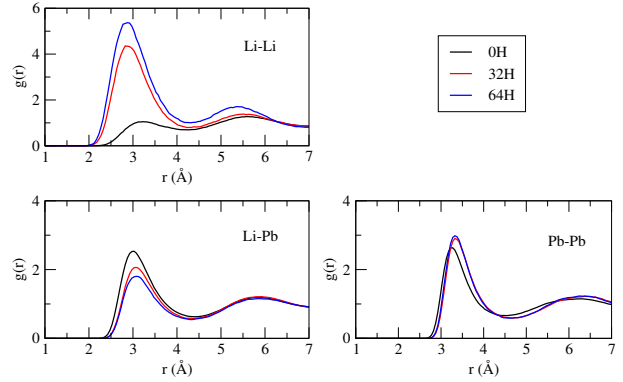


Figure 8: Partial correlation functions $g_{i,j}(r)$ of the three simulation systems with relatively low preassure at 775 K. The plots represents the pairs that involve only Li and Pb atoms.

H atoms were well separated from each other. Then the system was heated to 775 K, and let evolve. No molecules were formed at this stage. Then 83 per cent of the Li atoms were randomly selected and changed into Pb atoms, and the system was let to evolve. During this evolution, the first molecules were formed and after equilibration, the production run lead to the configurations considered in system 1. This resulted in an average number of 21 molecules (42 atoms of tritium in the molecular form) and 22 tritiums in atomic form.

The second system corresponds to a lower density and pressure but with the same nominal amount of T. In this case, the initial configuration was obtained by scaling the atomic coordinates to reflect the expansion of the system. This procedure moves atoms from their equilibrium positions (in particular molecules become elongated) and consequently, further equilibration then followed. Afterwards, the equilibrium configurations were generated in what we have defined as system 2. The average number of molecules did not change concerning system 1. Even so, their stability was observed to increase, being longer lived than at the higher pressure.

In the third step, the number of T atoms was halved, by removing 32 atoms selected randomly. Some of the deleted atoms were in atomic form and some were part of a molecule. Additionally, the coordinates were again scaled to take into account the variation in density needed to get a reasonable pressure. Of course, this required again further equilibration, leading finally to system 3, for which we generated the corresponding equilibrium configurations. In this case, the number of tritium molecules found was of 11.

Comparing the average number of molecules in the different simulations we obtained a similar proportion. For the 64 H case, we measured 21 tritium molecules (42 tritium atoms) for a total of 64 tritiums. In the 32H case, the number of molecules was 11 (22 tritium atoms) for a total of 32 tritiums. In all cases, therefore, around one third of the atoms stay in their atomic form and the others become part of a molecule. With this comparative study, we conclude that this proportion of atomic tritiums versus the total amount of T atoms present in

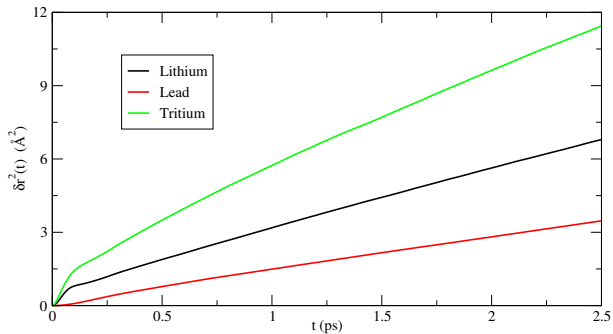


Figure 9: Mean squared displacement of the three different atoms corresponding to the third simulation case.

the simulation is independent of the number of tritium atoms, but of course, further studies with even fewer tritium atoms would be required to confirm if this situation holds.

iii. Dynamical properties

We have studied two main dynamical properties, the mean squared displacement (MSD) and the velocity autocorrelation function (VAF). Both of them are interesting, not only by themselves but for their potential use in the extraction of the diffusion coefficient parameter. This is one of the most important dynamical magnitudes, easy to obtain in simulations but hard (in cases like the present one, very hard) to get from experiments.

Mean squared displacement, MSD

The MSD is a property that measures how far and fast the atoms move away from their previous positions:

$$\delta r^2(t) = \langle (\vec{r}(t) - \vec{r}(0))^2 \rangle \quad (1)$$

Therefore, it measures the distance that an atom has travelled from the selected first point to the place where it is located after a time t has passed. It is interesting to signal that this magnitude presents clear differences between the different states of the matter. The gaseous state would present a similar qualitative aspect, but a clear different quantitative value, having a much more pronounced increase rate, related to the fast atomic diffusion that takes place in gases. In the crystalline solid case, the MSD would grow until the particles reach the maximum vibrational distance, so the global aspect of the plot would present an oscillatory shape.

We plot in figure 9 the mean squared displacement for the 32H simulational case. They show a typical shape for liquids, with an initial rapid rise and a long time linear behaviour, but not as pronounced as in gases. Tritium and lithium atoms even present some oscillation at short times, which can be interpreted as due to their collisions with the heavy Pb particles around them.

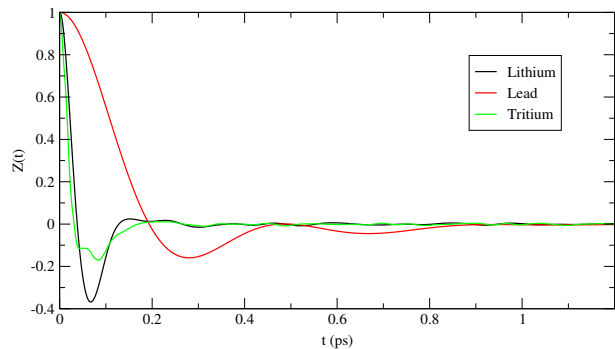


Figure 10: Velocity autocorrelation function of the three different atoms corresponding to the third simulation case.

The behaviour for the different types of atoms is what we could expect in a system like this one with different atomic masses. The slope of the curves increases when the mass of the atoms decreases. The diffusion coefficient is related with the MSD by the equation:

$$D = \lim_{t \rightarrow \infty} \frac{1}{6} \frac{d\delta r^2(t)}{dt} \quad (2)$$

So, the slope of the MSD curve at long times gives the value of the diffusion coefficient. Table 5 shows a comparison between all the diffusion coefficients in all the simulated cases.

Velocity autocorrelation function, VAF

The VAF measures the variation in the direction of the velocity of a particle as a function of time:

$$Z(t) = \frac{\langle \vec{v}_i(t) \cdot \vec{v}_i(0) \rangle}{\langle \vec{v}_i(0)^2 \rangle} \quad (3)$$

This magnitude is related to how hard is for an atom to change its direction of movement. This magnitude is notably influenced by the mass of the atoms. Heavier atoms present a bigger momentum than the lighter ones, and that makes it harder for them to change their direction of movement compared to lighter atoms, that are much more easily influenced by collisions with the heavier ones. Consequently, it is expected that the time variation of the VAF of T and Li will be more rapid than that corresponding to Pb atoms.

Table 5: Diffusion coefficient of the atoms through all the different studied cases as obtained from the MSD.

Diffusion coefficient from MSD				
Atoms	1- 64H	2- 64H	3- 32H	4- 0H
Li	0.085	0.406	0.402	0.510
Pb	0.04	0.187	0.216	0.326
T	0.200	0.427	0.625	-

Table 6: Diffusion coefficient of the atoms through all the different studied cases obtained from VAF.

Diffusion coefficient from VAF in $\text{\AA}^2/\text{ps}$				
Atoms	1- 64H	2- 64H	3- 32H	4- 0H
Li	0.084	0.361	0.357	0.522
Pb	0.038	0.196	0.213	0.333
T	0.200	0.435	0.572	-

Figure 10 shows the graphs representing the VAF function for the different atoms in the 32H simulation case. The different plots present as expected a clear difference depending on the mass of the atoms. As a general rule $Z(t)$ oscillates and gets damped for increasing times. However, in the case of T, small amplitude and high-frequency oscillations appear superimposed on this global behaviour. We will later comment on the frequency of these oscillations and their origin.

The velocity correlation function is also related to the diffusion coefficient by the following function:

$$D = \frac{k_B T}{m} \int_0^\infty Z(t) dt \quad (4)$$

Table 6 shows the diffusion coefficient values extracted from the VCF. The results compare well with those obtained from the MSD, previously represented in table 5, which reassures the internal consistency of our simulations.

The first aspect to consider about the diffusion coefficients is their comparison with experiment. According to the formula presented by Kobayashi et al, deduced from their experimental data [35], the D coefficient of T for our temperature conditions would be $D = 0.67 \text{\AA}^2/\text{ps}$. As we already said in the introduction, there is some dispersion between the different diffusivity results, and according to Terai et al [22], the value would be $D = 0.38 \text{\AA}^2/\text{ps}$. Our obtained value at low pressure conditions (simulations 2 and 3) is located between Terai's and Kobayashi's ones. For the Li and Pb atoms in a combination with T, there is no available experimental data. It would have been interesting to compare our results for the atomic diffusivities with those obtained in the only other ab initio study of the LiPbH system where one single H atom was considered [30], but unfortunately, no such values were reported.

Concerning the pure eutectic LiPb alloy (system 4) there are some classical simulations available that can be compared to ours. Gan et al. [42] gives the values $D = 0.3 \text{\AA}^2/\text{ps}$ for lead and $D = 0.5 \text{\AA}^2/\text{ps}$ for lithium, which are very similar to our values.

Another interesting aspect is the variation of the diffusion coefficients with thermodynamic conditions, i.e. with pressure and with tritium content. In tables 5 and 6 we observe that the diffusivities of Li and Pb decrease when T is added. There are several possible reasons for this behaviour. First, it is observed that the

densities are higher in the presence of T, and consequently the volume per atom decreases. Therefore, each atom has, so to say, less available space to move, and this contributes to a decrease in mobility. The second possible cause that affects the mobility of the atoms is the presence of new bonds, in this case with T. Gan et al [42] also found a decrease in the mobility of the atoms in the PbLi alloy as compared to the pure components, and attributed this change to the bonds between Li atoms and Pb atoms. In fact, the D coefficient of Li suffered a more severe reduction from the pure metal to the alloy, which is related to the high number of Pb first neighbours, whereas the reduction was much less important in the case of the lead, being the majority atoms in the composition, with few lithiums as first neighbours. The situation is similar in our study, and it can clearly be seen in the fourth case. The inclusion of T, on the other hand, leads to new bonds and a corresponding reduction in the diffusion coefficients of Li and Pb.

The differences brought about by increasing the pressure are related to the density effect, because of the substantial reduction of the atomic volume.

An advantage of the VAF over the MSD is that with VAF we can calculate the vibrational frequencies of the different atoms, by simple application of a Fourier transform to the VAF data, leading to the so called power spectrum, $Z(\omega)$ where the typical vibrational frequencies of the atoms appear as peaks.

Vibrational Frequencies

Figure 11 represents the power spectrum for the three types of atoms in simulation 2, with 64 tritium atoms. We find an obvious lower frequency peak for Pb atoms, and peaks for Li and T at a similar frequency, which somehow reinforces the idea that the interaction between Li and T is quite strong, producing a kind of coupled oscillatory motions. Taking a close look at the tritium power spectrum we can also observe a small peak at around 400 ps^{-1} , which is not present in the curves of the other atoms. This is a direct consequence of the fast oscillations observed in the corresponding $Z(t)$ of T commented above. We assign this small peak to the high frequency vibration of the tritium molecules present in the sample.

In order to check that this is indeed the case, we studied the time evolution of the interatomic distance between the T atoms in the molecules that were present in the simulation. This was Fourier Transformed and the results for all the molecules were then averaged.

Figure 12 shows these averages between all the vibrational frequencies of the molecules for the three systems where T is present. As we can see, the distribution of frequencies presents a clear peak at a frequency

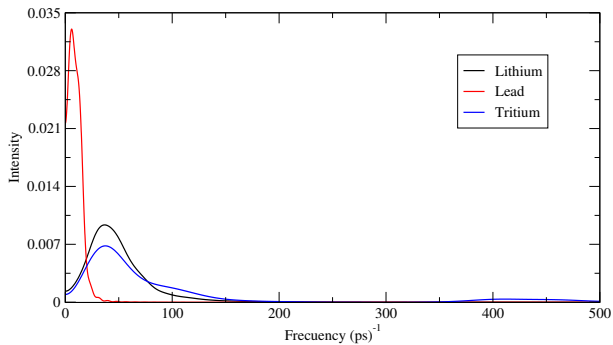


Figure 11: *Spectrum of frequencies corresponding to Pb, Li and T, at the second simulation state (2-64H).*

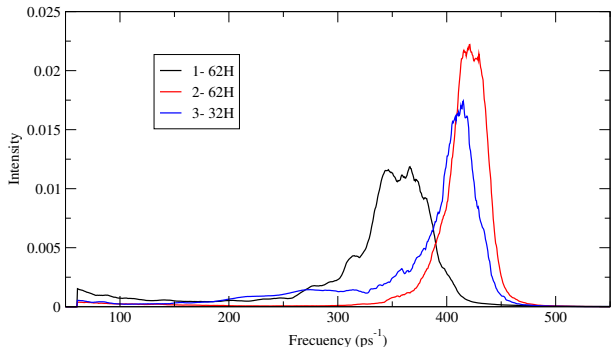


Figure 12: *Molecular frequencies of the atoms for the first three simulation cases.*

somewhat above 400 ps^{-1} for the low-pressure cases, and around 350 ps^{-1} for the high-pressure case.

In principle, this change could be thought to be a direct consequence of pressure, but since we are talking about an intrinsic property of the molecules this direct relation does not look reasonable, and a more indirect effect must be the cause.

The particular aspect related to T_2 molecules that we have found to be different between the low and the high-pressure states, that could affect the molecule vibrations is the distribution of Li atoms around. As we observed in table 4 the distance to from T_2 molecules to Li atoms decreases substantially for the higher pressure. Therefore, we can conclude that the interaction of Li atoms with tritium molecules is also strong (as was the case with T in atomic form) leading to an important modification of the properties of the molecule, at least as far as its vibrations are concerned, when they are near them.

IV. CONCLUSIONS

In this work, we have carried out an in-depth first principles simulation study of the proposed lithium-lead TOKAMAK's blanket atomic structure and dynamic properties.

The distribution of the atoms has been analyzed in detail, and the appearance of tritium molecules has required a more detailed analysis of the structural proper-

ties. We have observed that the first coordination shell of Li atoms is composed of T atoms and, in smaller quantity, tritium molecules. This underlies the strength of Li interactions with T, which entails an induced increase in the Li-Li interactions and consequently, a large variation in their coordination as compared to the pure eutectic where no T is present. An additional effect observed is a kind of coupling of the atomic vibrations of Li and T atoms, as evidenced by a similar vibration frequency of both types of atoms. Moreover, the importance of the interactions between Li and tritium molecules is also evidenced by the significant change in the molecular vibration frequency when they get closer to Li atoms as a consequence of applying pressure.

Pb atoms, on the other hand, are not much influenced by the presence of T, and their characteristic properties hardly change.

Finally, we have analyzed in detail the particle distribution around T atoms and T_2 molecules, and their variations with thermodynamic conditions. The decrease in pressure, and correspondingly in density, leads not only to an expansion in the typical distances but also to a more diffuse structure where coordination shells get wider and lower. In the particular case of tritium molecules, this leads to a very diffuse distribution of atoms around them, where no first coordination shell could be defined.

Concerning the dynamical properties, we focused our attention on the MSD, the FAV and the D coefficient. For the MSD we were able to identify a clear inverse dependency between the slope and the mass of the atoms. The behaviour shown by the mean squared displacement of the atoms is inbetween that of solids and gases. The curves exhibit a linear increase for long times, not like the solids, which come back and forth because their mobility is restricted to the vibrational modes and they can't move from their equilibrium position. But at the same time, the slope is not very pronounced and even tritium and lithium present a kind of first peak at the beginning of the curves, which would never appear in a gaseous MSD.

For the VAF function, it happens something similar to the MSD. The solid's VAF typical behaviour consists of a purely oscillatory curve. The gaseous behaviour, in contrast, shows no oscillations but a fast decrease towards zero. Our results are once again, inbetween solid and gaseous behaviour, with small oscillations with decreasing amplitude as the time passes. With both the velocity autocorrelation function and the mean squared displacement, we could extract a value for the diffusion coefficient of the atoms (D).

The diffusion coefficients for the different atoms indicated higher mobility of the lighter atoms and a lower one for the heavier atoms. This can be expected in this type of system, and the major importance of this parameter comes from the comparison between systems with different thermodynamic conditions. We have observed that reduced atomic volume (increased density) and an increased number of bonds can explain the ob-

served variation of the diffusion coefficients.

We have also obtained good agreement with different proposed values as extracted from the experiment, but could not compare to other simulation studies because there are no values of D reported for this type of system.

We end up by indicating that if the TOKAMAK's blanket has a sufficient amount of tritium atoms for them to be able to stay in close contact, around two thirds of the tritium atoms will form bonds with other tritiums and will constitute a molecule. This is a prominent conclusion, as the formation of molecules can affect significantly the extraction of the tritium from the blanket to the plasma, which is essentially the main function of the blanket, as we explained in the introduction.

An expected aspect we wanted to study but we could not finally perform, is the inclusion of He atoms in the same amount as tritium ones, that would be formed during the breeding reaction. This is left for future research. Another interesting aspect to analyze is how properties would change for decreasing the amount of tritium present, and how they would evolve towards the results at infinite dilution, closer to the only previous first principles study of this type of system.

V. ACKNOWLEDGEMENTS

I would like to thank my advisor, D. Luis Enrique Gonzalez Tesedo, for his patience with all my different questions and requests, which he had already provided but nerve minded repeating. This article is finished thanks to him and to D. David J. Gonzalez Fernandez passionate teaching.

REFERENCES

- [1] V. Coen. "Lithium-lead eutectic breeding material in fusion reactors". Journal of Nuclear Materials, 133 & 134 (1985), pages, 46-51.
- [2] Heriberto Pfeiffer. "Lithium. Technology, performance and safety nova science". Phd Thesis, Universidad Autónoma de México, Mexico D.F. (2014), Chapter 8, pag 226.
- [3] S. Malang, R. Mattas. "Comparison of lithium and the eutectic lead-lithium alloy, two candidate liquid metal breeder materials for self-cooled blankets". Fusion Engineering and Design, 27 (1995), pages. 399-406.
- [4] F. A. Hernández, P. Pereslavitsev. "First principles review of options for tritium breeder and neutron multiplier materials for breeding blankets in fusion reactors". Fusion Engineering and Design, 137 (2018), pages. 243-256.
- [5] Belit Garcinuño Pinado. "Design of an experimental facility for tritium extraction from eutectic lead-lithium". Phd Thesis, UNED, Madrid (2018), . . .
- [6] S. Fukada, Y. Edao, S. Yamaguti, T. Norimatsu. "Tritium recovery system for Li-Pb loop of inertial fusion reactor". Fusion Engineering and Design, 83 (2008), pages. 747-751.
- [7] W. Farabolini, A. Ciampichetti, F. Dabbene, et al. "Tritium control modelling for a helium cooled lithium-lead blanket of a fusion power reactor". Fusion Engineering and Design, 81 (2006), pages. 753-762.
- [8] J.P. Catalán et al. "Neutronic analysis of a dual He/LiPb coolant breeding blanket for DEMO". Fusion Engineering and Design, 86 (2011), pages. 2293-2296.
- [9] T. Hasegawa, Y. Yamamoto and S. Konishi. "Conceptual design of advanced blanket using liquid LiPb". IEEE 22nd Symposium of Fusion Engineering (2007).
- [10] S. Fukada, T. Terai, S. Konishi, K. Katayama, T. Chikada, Y. Edao, T. Muroga, M. Shimada, B. Merrill and D. K. Sze. "Clarification of tritium behavior in Pb-Li blanket system". Materials Transactions, 54 (2013), pages. 425-429.
- [11] Sanjay Kumar, Amit Tirpude, Nagaiyar Krishnamurthy. "Studies on the solubility of hydrogen in molten $Pb_{83}Li_{17}$ eutectic alloy". International Journal of Hydrogen Energy, 38 (2013), pages. 6002-6007.
- [12] A. Fraile, S. Cuesta-López, A- Caro, D. Schwen and J. M. Perlado. "Interatomic potential for the compound-forming Li-Pb liquid alloy". Journal of Nuclear Materials, 448 (2014), pages. 103-108.
- [13] Henner Ruppertsberg and Walter Speicher. "Density and Compressibility of Liquid Li-Pb Alloys". Z. Naturforsch, 31a (1976), pages. 47-52.
- [14] H. Ruppertsberg and J. Jost. "Determination of the heat capacity of liquid alloys according to the $(dp/dt)_S$ procedure: Pb/Na". Thermochemica Acta, 151 (1989), pages. 187-195.
- [15] Y. Senda et al. "The ionic structure and the electronic states of liquid Li-Pb alloys obtained from ab initio molecular dynamics simulations". Journal of Physics: Condensed Matter, 12 (2000), 6101.
- [16] C. H. Wu. "The interaction of hydrogen isotopes with lithium-lead alloys". Journal of Nuclear Materials, 122 & 123 (1984), pages. 941-946.
- [17] H. Ruppertsberg and H. Egger. "Short-range order in liquid Li-Pb alloys". J Chem. Phy. 63 (2008), 4095.

- [18] E. Mas de les Valls et al. "Lead-lithium eutectic material database for nuclear fusion technology". Journal of Nuclear Materials, 376 (2008), pags. 353-357.
- [19] M. Okada, Y. Edao, H. Okitsu and S. Fukada. "Analysis of simultaneous H and D permeation through lithium-lead". Plasma and Fusion Research: Regular Articles, 7 (2012), 2405074.
- [20] F. Reiter. "Solubility and diffusivity of hydrogen isotopes in liquid Pb-17Li". Fusion Engineering and Design, 14 (1991), pags. 207-211.
- [21] Y. Maeda, Y. Edao, S. Yamaguchi and S. Fukada. "Solubility, diffusivity and isotopic exchange rate of hydrogen isotopes in Li-Pb". Fusion Science and Technology, 54 (2008), pags. 131-134.
- [22] T. Terai et al. "Diffusion coefficient of tritium in molten lithium-lead alloy ($Li_{17}Pb_{83}$) under neutron irradiation at elevated temperatures". Journal of Nuclear Materials, 187 (1992), pags. 247-253.
- [23] R. M. Alire. "Transport of hydrogen in liquid lithium". Journal of Chemical Physics, 65 (1976), 1134.
- [24] S. Fukada, M. Kinoshita, K. Kuroki, T. Muroga. "Hydrogen diffusion in liquid lithium from 500 °C to 600 °C". Journal of Nuclear Materials, 346 (2005), pags. 293-297.
- [25] D. Martelli, A. Venturini and M. Utili. "Literature review of lead-lithium thermophysical properties". Fusion Engineering and Design, 138 (2019), pags. 183-195.
- [26] D. K. Belashchenko et al. "Application of the embedded atom model to liquid metals: Liquid lithium". High Temperature, 47 (2009), pags. 211-218.
- [27] D. K. Belashchenko. "Embedded atom method potentials for alkali metals". Inorganic Materials, 48 (2012), pags. 79-86.
- [28] Y. Wu and the FDS Team. "Conceptual design and testing strategy of a dual functional lithium-lead test blanket module in ITER and EAST". Nuclear Fusion, 47 (2007), 1533-9.
- [29] A. Fraile and T. Polcar. "Volume and pressure of helium bubbles inside liquid Pb16Li. A molecular dynamics study". Nuclear Fusion, 60 (2020) 046018.
- [30] Daisuke Masuyama et al. "Chemical state and diffusion behavior of hydrogen isotopes in liquid lithium-lead". Chemical Physics Letters, 483 (2009), pags. 214-218.
- [31] Joël Martín. "Estudio de primeros principios de la estructura y difusión de tritio en la aleación líquida de litio-plomo". TFG, Valladolid, (2019). <http://uvadoc.uva.es/handle/10324/38273>
- [32] J. Souto, M.M.G. Alemany, L.J. Gallego, L.E. Gonzalez and D. J. Gonzalez. Unpublished.
- [33] S. Fukada, T. Muneoka, R. Yoshimura, K. Katayama, Y. Edao and T. Hayashi. "Recovery of hydrogen isotopes by liquid-gas contactor from $Li_{17}Pb_{83}$ blanket". J. Plasma Fusion Res. SERIES, 11 (2015).
- [34] P. Hubberstey, T. Sample and M. G. Barker. "Is Pb-17Li really the eutectic alloy? A redetermination of the lead-rich section of the Pb-Li phase diagram ($0.0 < x_{Li} < 22.1$ at%)". Journal of Nuclear Materials, 191-194 (1992), pags. 283-287.
- [35] M. Kobayashi et al. "Kinetics of tritium release from thermal neutron-irradiated $Li_{0.17}Pb_{0.83}$ ". Fusion Science and Technology, 62 (2017), pags. 56-60.
- [36] G. Grube and H. Klaiber. "Elektrische Leitfähigkeit und Zustandsdiagramm bei binären Legierungen". Z. Elektrochem., 40 (1934), 745.
- [37] G. Kresse G. and J. Hafner. "Ab initio molecular dynamics for liquid metals". Phys. Rev. B, 47 (1993), 558.
G. Kresse G. and J. Hafner. "Ab initio molecular-dynamics simulation of the liquid-metal-amorphous-semiconductor transition in germanium". Phys. Rev. B, 49 (1994), 14251.
G. Kresse G. and J. Furthmüller. "Efficiency of ab-initio total energy calculations for metals and semiconductors using a plane-wave basis set". Comput. Mater. Sci., 6. (1996), 15.
- [38] J. P. Perdew, K. Burke and M. Ernzerhof. "Generalized Gradient Approximation Made Simple". Phys. Rev. Lett., 77 (1996), 3865.
- [39] P. E. Blöchl. "Projector augmented-wave method". Phys. Rev. B, 50 (1994), 17953.
G. Kresse and D. Joubert. "From ultrasoft pseudopotentials to the projector augmented-wave method". Phys. Rev. B, 59 (1999) 1758.
- [40] V. Milman et al. "Electronic structure, properties, and phase stability of inorganic crystals: A pseudopotential plane-wave study". International Journal of Quantum Chemistry, 77 (2000) 5.
- [41] Y. Waseda. "The structure of non crystalline materials: liquids and amorphous solids". (1980).
- [42] X. Gan, S. Xiao, et al. "Thermodynamic properties of Li, Pb and $Li_{17}Pb_{83}$ with molecular dynamics simulations". Fusion Engineering and Design, 89 (2014), pags. 2946-2952.